15 Challenges from Experiment: Correlation Effects and Electronic Dimer Formation in Ti_2O_3

T. C. Koethe and L. H. Tjeng
University of Cologne
Max Planck Institute for Chemical Physics of Solids
Dresden

Contents

E. Pavarini, E. Koch, D. Vollhardt, and A. Lichtenstein
DMFT at 25: Infinite Dimensions
Modeling and Simulation Vol. 4
Forschungszentrum Jülich, 2014, ISBN 978-3-89336-953-9
http://www.cond-mat.de/events/correl14

1 Introduction

The spectacular physical properties often observed in materials containing transition-metal and rare-earth elements challenge our comprehension of solid state physics [1, 2]. These properties include superconductivity, unusually large magnetoresistance, metal-insulator transitions, and multiferroicity. We would like to understand how the electrons in such materials interact with each other as to generate those unusual quantum phenomena. From a theoretical viewpoint, it turns out that the equations we have to solve are so complicated that we will not be able to obtain exact solutions. To make things worse and more fascinating at the same time, tiny changes in temperature, pressure, or in the material composition may cause large changes of the properties so that it appears that there are many solutions available that lie very close together in energy. With exact solutions out of reach, the objective is to find smart approximations by which we can capture the essential physics to describe the correlated motion of the electrons in such materials. It may very well be that we need to develop and use different approximations for different materials or properties.

In order to test the validity and accuracy of the theoretical approximations, one can utilize photoelectron spectroscopy [3, 4] as a powerful tool to unravel the electronic structure of the material. One can use the extremely large dynamic range in energy: by studying excitation spectra in the energy range from several eV up to several hundreds of eV, one can obtain direct information about the "bare" electrons, e.g. the charge, spin, and orbital state of the ions that make up the correlated material. By measuring the excitation spectra in the vicinity of the chemical potential with ultra-high resolution, one can directly find the momentum-dependent behavior of the "dressed" electrons, i.e. quasiparticles.

In the following, we will address a long-standing issue concerning the electronic structure of Ti_2O_3. The basic crystal structure and relevant orbitals are shown in Fig. 1. This material is a non-magnetic insulator at low temperatures and shows a gradual insulator-to-metal transition with metal-like conductivity for temperatures above 500 K [6–10]. The transition is not accompanied by a change in symmetry of the crystal structure [11]. Band structure calculations have great difficulties explaining the properties of this compound: the low temperature phase is calculated to be a metal rather than an insulator [12, 13]. Cluster methods were used to explain the insulating state and the transition by involving, among others, an on-site (intra Ti $3d$) correlation energy [14–16].

Several photoelectron spectroscopic experiments have been carried out on the Ti core levels and the valence band [17–23], thereby identifying the O $2p$ and Ti $3d$ derived character of the valence band and establishing the insulating character of the compound in the low temperature phase. Strangely enough, none of these reported photoemission studies have revealed the presence of satellite structures that otherwise would be consistent with the formation of the c-axis dimers in the low-temperature phase as proposed by the cluster studies [14–16, 24]. The structural presence of the c-axis dimers can be seen in Fig. 1.

Here we will revisit the valence band photoemission experiment with the emphasis on obtaining spectra that are representative for the bulk material. We will analyze the spectra on the basis

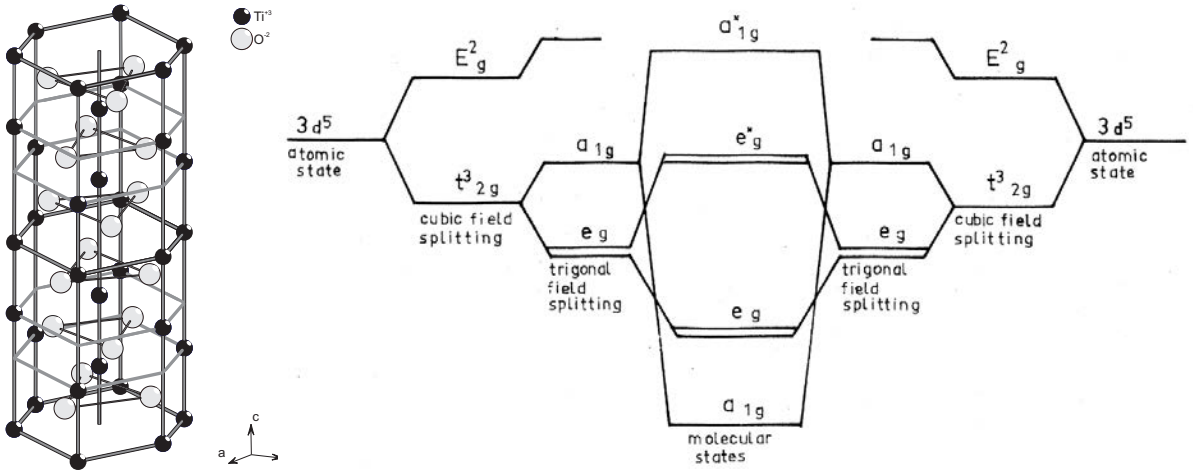

Fig. 1: *(Left) Corundum structure of Ti_2O_3 at $T = 300\,K$ in the insulating phase. Titanium (oxygen) sites are indicated by black (white) spheres. (Right) Energy level diagram adapted from Castellani et al. [5] for a c-axis dimer of titanium sites. One-electron orbitals of each site are shown on the left and right sides, with the resulting molecular orbitals in the center.*

of the hydrogen molecule model, thereby establishing not only that the c-axis dimer is present *electronically*, but also quantifying the importance of correlation effects relative to the *intra-dimer hopping* for the gap formation in the low temperature phase.

2 Experimental

Single crystals of Ti_2O_3 were grown by H. Roth (University of Cologne) using a floating-zone mirror furnace and subsequently characterized by x-ray diffraction and thermogravimetric analysis. No impurities or foreign phases in the samples were detected, which was also confirmed by the photoemission measurements. These measurements were taken at room temperature on *in-situ* cleaved samples. The photoemission spectra (in the following referred to as XPS) were collected using a VG twin-crystal monochromatized Al K_α x-ray source with h$\nu = 1486.6\,$eV and a Scienta SES 100 hemispherical electron energy analyzer. The overall experimental energy resolution was set to 350 meV. The pressure in the spectrometer chamber was below 2×10^{-10} mbar during the measurement. The possible process of aging of the sample was monitored by repeated O $1s$ spectra alternating with the measurement of the valence band region. No significant changes during the entire experiment (48 h) were observed.

3 Results

The room temperature XPS valence band spectrum is shown in Fig. 2. The large spectral weight at 4–10 eV binding energies can be attributed to bands with mainly O $2p$ character. The lower energy region from the Fermi level up to 4 eV consists of mainly Ti $3d$ contributions. This part of the spectrum is characterized by two distinct structures. The main line (M) is a sym-

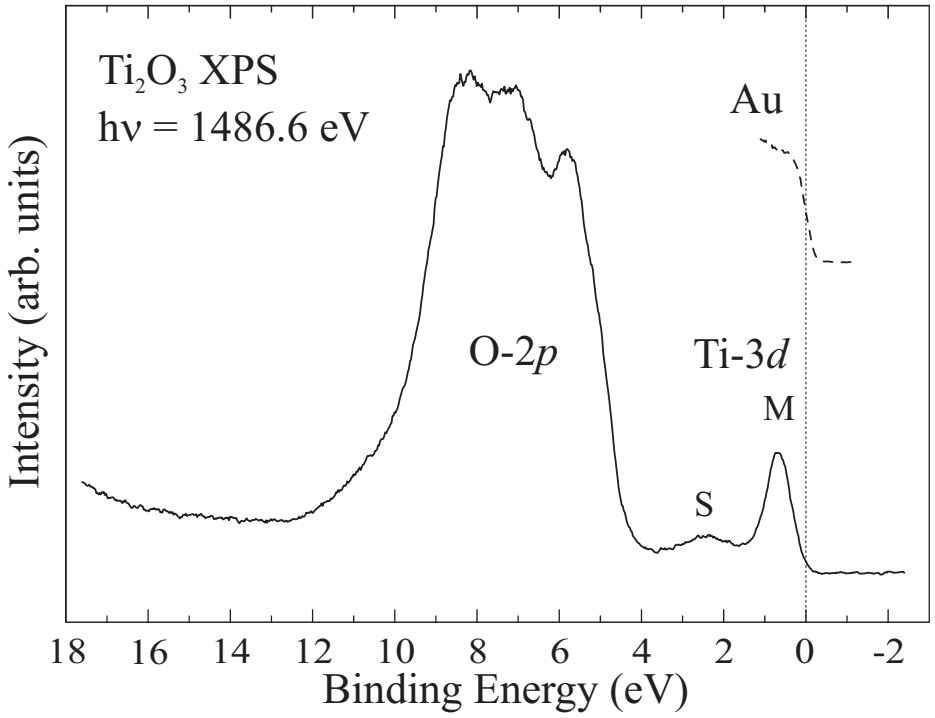

Fig. 2: *Room temperature valence band photoemission spectrum of Ti_2O_3 taken at 1486.6 eV photons. The Fermi level was calibrated using a polycrystalline gold sample shown by the dashed line.*

metric peak with a width of ≈ 0.8 eV FWHM centered at about 0.7 eV. The semiconducting or insulating nature of the system at room temperature [7–9] is reflected by the fact that the spectral weight vanishes close to the Fermi level, in agreement with earlier photoemission reports [17–22]. The second feature is a weak but clearly noticeable satellite (S) at around 2.4 eV binding energy. The existence of this satellite has not been reported in the literature before [17–22].

One of the concerns with respect to the results reported in the literature is related to the surface sensitivity of photoelectron spectroscopy when using low photon energies. One can estimate that the probing depth is no more than 7–10 Å for ultraviolet photons. At 1486.6 eV, the probing depth is estimated to be around 20 Å, and apparently, this is needed to observe the existence of the satellite (S).

4 Discussion: the Hubbard model for the hydrogen molecule

Establishing the presence of the satellite (S) structure is essential for identifying the appropriate model for Ti_2O_3. Band theory not only fails to produce a gap at the Fermi level, but also does not reveal any structure in the calculated density of states in the 1–3 eV binding energy region [12, 13]. Only the main line (M) is reproduced. It is also important to note that single-site cluster approaches that include correlation effects do not produce a satellite structure in

the 1–3 eV region, only the main line appears in the calculations [21, 22, 16]. We therefore infer that the satellite (S) structure can only be explained if two aspects are taken into account simultaneously: correlation effects and strong intra-dimer hopping [15, 16]. To demonstrate this point, we now will simulate the Ti $3d$ derived features using the Hubbard model for the hydrogen molecule [25], where the H $1s$ orbital is representing the occupied Ti $3d$ a_{1g} orbital as illustrated in Fig. 1 and indicated experimentally by XAS measurements [24].

4.1 Ground state

The model consists of two electrons that can be distributed over two sites denoted by $i = 1, 2$. The ground state $|GS\rangle$ of the system can be described as a linear combination of a state $|\varphi_0\rangle$ in which the two electrons are on different sites coupled to a singlet, and another singlet state $|\varphi_1\rangle$ in which both electrons are on the same site,

$$\begin{aligned} |GS\rangle &= \alpha|\varphi_0\rangle + \beta|\varphi_1\rangle \\ |\varphi_0\rangle &= \frac{1}{\sqrt{2}}\left(c^\dagger_{1\uparrow}c^\dagger_{2\downarrow} + c^\dagger_{2\uparrow}c^\dagger_{1\downarrow}\right)|0\rangle \\ |\varphi_1\rangle &= \frac{1}{\sqrt{2}}\left(c^\dagger_{1\uparrow}c^\dagger_{1\downarrow} + c^\dagger_{2\uparrow}c^\dagger_{2\downarrow}\right)|0\rangle. \end{aligned}$$

Here, $|0\rangle$ denotes the vacuum state out of which the operators $c^\dagger_{i\sigma}$ create an electron at site i with spin $\sigma =\uparrow, \downarrow$. The triplet states are not considered since they do not hybridize with each other to allow for the formation of a lower energy state [25]. The coefficients α and β are determined by diagonalizing the ground state Hamiltonian,

$$\mathcal{H}_{GS} = \begin{pmatrix} 0 & 2t \\ 2t & U \end{pmatrix},$$

in which U denotes the on–site Coulomb repulsion between two electrons at the same site, and t the hopping integral of the electron between the two sites. The energy of the ground state is then given by

$$E_0 = \frac{1}{2}\left(U - \sqrt{U^2 + 16t^2}\right) .$$

4.2 Photoemission final states

The photoemission process, in which an electron is removed, is represented by the annihilation operators $c_{i\sigma}$. In a basis of states in which the remaining electron is localized at one of the two sites, $c^\dagger_{i\sigma}|0\rangle$, $i = 1, 2$, the final state Hamiltonian and the corresponding eigenstates are given by

$$\mathcal{H}_{FS} = \begin{pmatrix} 0 & t \\ t & 0 \end{pmatrix},$$

$$|FS^\pm\rangle = \frac{1}{\sqrt{2}}\left(c^\dagger_{1\sigma} \pm c^\dagger_{2\sigma}\right)|0\rangle.$$

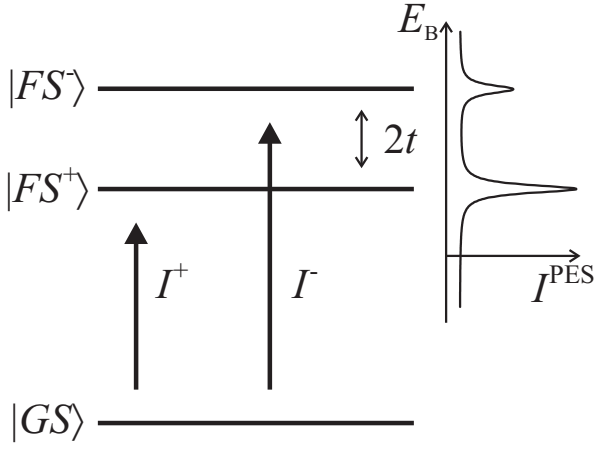

Fig. 3: *Total energy level diagram for the photoemission process in a hydrogen molecule model. The two accessible final states $|FS^+\rangle$ and $|FS^-\rangle$ yield two lines in the spectrum of intensities I^+ and I^-, respectively, according to the initial state coefficients α and β. The corresponding spectrum is indicated on the right.*

These final states are the well known bonding and anti-bonding states of the H_2^+ ion which are separated in energy by $2t$. See Fig. 3.

4.3 Photoemission spectral weights

Depending on the spin of the removed photoelectron, the final states can take two spin orientations σ of equal energy. One can see immediately that the photoemission spectrum of this system consists of two lines associated with the two final states. The separation of the peaks in the spectrum is given by the final state splitting $2t$. Their intensities depend only on the initial state coefficients α and β. A qualitative spectrum is sketched in Fig. 3 on the right with a lifetime broadening of the photoemission lines taken into account.
We calculate the spectrum as the intensity proportional to the square of the transition matrix elements for the photoemission process,[1]

$$\begin{aligned} I^{\pm} &\propto \|\langle FS^{\pm}|c_{i\sigma}|GS\rangle\|^2 \\ &= \frac{1}{4}|\alpha \pm \beta|^2 \\ &= \frac{1}{4}\left(1 \pm \sqrt{16t^2/\left(U^2+16t^2\right)}\right). \end{aligned}$$

We thus find that the intensities only depend on the ratio between U and t, and we can immediately evaluate the relative intensities for two limiting cases. Firstly, for $U = 0$, I^- vanishes, and the spectrum will be given by a single line only. In other words, although there are two final

[1]Note that the sum of I^+ and I^- equals 1/4 instead of 1. Since there are four photoemission operators $c_{i\sigma}$ for $i = 1, 2$ and $\sigma = \uparrow, \downarrow$, which naturally all yield the same intensities, the total intensity equals 1.

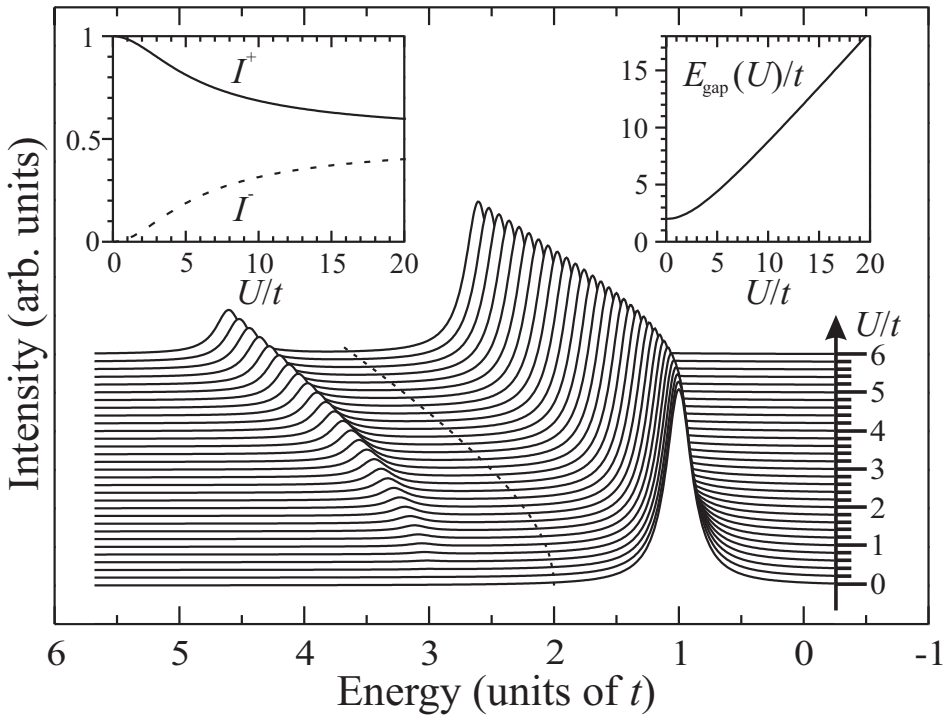

Fig. 4: *Calculated photoemission spectra of the hydrogen molecule model in energy units of* t *for* $0 \leq U/t \leq 6$ *with a lifetime broadening of* $0.25t$*. Left inset: the variation of* I^+ *(solid line) and* I^-*(dashed) with* U/t*. Right inset: the energy gap in units of* t *as function of* U/t*.*

states, we can only reach the lowest of them due to the fully constructive and fully destructive interference ($\alpha = \beta$ when $U = 0$) in the expression for the transition matrix elements. We are thus back to the one-electron approximation and reproduce essentially the results of band structure calculations. Secondly, for $U/t \to \infty$, the intensities for the two final states become equal: the satellite intensity I^- is as large as that of the main line I^+. In this limit, there is no double occupation in the ground state and the two electrons reside on one site each ($\alpha = 1$ and $\beta = 0$).

In Fig. 4, we show the intensities for a range of U/t values. The energy scale is in units of t. The energy scale is chosen such that the zero, given by the chemical potential μ, lies in the center of the energy gap shown in the right inset. The gap is given by

$$E_{gap} = \sqrt{U^2 + 16t^2} - 2|t| \; .$$

One can clearly see how the satellite intensity I^- grows with increasing U/t. Comparing the H_2 model calculations as shown in Fig. 4 with the experimental spectrum for Ti_2O_3 as displayed in Fig. 2, we can make the estimate from the experimental satellite to main line intensity ratio that $U/t \approx 3 - 4$. The experimental energy separation between the satellite and the main line is $2.4 - 0.7 = 1.7\,$eV, which corresponds with $2t$ in the hydrogen model. We thus obtain the estimate that $t \approx 0.85\,$eV and $U \approx 2.5 - 3.4\,$eV for Ti_2O_3.

5 Conclusions

We have investigated the low temperature phase of Ti_2O_3 with bulk sensitive photoelectron spectroscopy. We find a distinct two-peak structure in the Ti $3d$ contribution to the valence band spectrum. We attribute this to correlation effects at the Ti $3d$ and to the presence of inter-site hopping within the c-axis dimer. On the basis of the Hubbard model for the hydrogen molecule, we can make realistic estimates for the magnitude of the Hubbard U and the intra-dimer hopping intergral t. We can conclude that the c-axis dimers exist not only structurally but also electronically. This finding is relevant for a better understanding of the insulator-to-metal transition, in which an electronic break-up of the c-axis dimers for the high temperature phase can be hypothesized.

Acknowledgements

The research is supported by the Deutsche Forschungsgemeinschaft through SFB608 and FOR 1346. We would like to thank L. Hamdan for her skillful technical and organizational assistance and J. Weinen for his assistance in preparing this manuscript.

References

[1] for a review see: Electronic Conduction in Oxides by N. Tsuda, K. Nasu, A. Yanase, and K. Siratori, Springer Series in Solid-State Sciences 94, (Springer Verlag, Berlin 1991)

[2] for a review see: M. Imada, A. Fujimori, and Y. Tokura, Rev. Mod. Phys. **70**, 1039 (1998)

[3] C.-O. Almbaldh and L. Hedin, *Handbook on Synchrotron Radiation*, Vol. 1b, ed. by E.E. Koch, (North-Holland, Amsterdam, 1983) p. 607

[4] for a review see: S. Hüfner: *Photoelectron Spectroscopy*, Springer Series in Solid-State Sciences, Vol. 82, (Springer Verlag, Berlin 1996)

[5] C. Castellani, C.R. Natoli, and J. Ranninger, Phys. Rev. B **18**, 4945 (1978)

[6] L.K. Keys and L.N. Mulay, Phys. Rev. **154**, 453 (1967)

[7] L.L. van Zandt, J.M. Honig, and J.B. Goodenough, J. Appl. Phys. **39**, 594 (1968)

[8] J.M. Honig and T.B. Reed, Phys. Rev. **174**, 1020 (1968)

[9] J.M. Honig, Rev. Mod. Phys. **40**, 748 (1968)

[10] R.M. Moon, T. Riste, W.C. Koehler, and S.C. Abrahams, J. Appl. Phys. **40**, 1445 (1969)

[11] C.E. Rice and W.R. Robinson, Acta Cryst. B **33**, 1342 (1977)

[12] L.F. Mattheiss, J. Phys.: Condens. Matter **8**, 5987 (1996)

[13] V. Eyert, U. Schwingenschlögl, and U. Eckern, Europhys. Lett. **70**, 782 (2005)

[14] H. Nakatsugawa and E. Iguchi, Phys. Rev. B **56**, 12931 (1997)

[15] A. Tanaka, J. Phys. Soc. Jpn. **73**, 152 (2004)

[16] A.I. Poteryaev, A.I. Lichtenstein, and G. Kotliar, Phys. Rev. Lett. **93**, 086401 (2004)

[17] R.L. Kurtz and V.E. Henrich, Phys. Rev. B **25**, 3563 (1982)

[18] J.M. McKay, M.H. Mohamed, and V.E. Henrich, Phys. Rev. B **35**, 4304 (1987)

[19] K.E. Smith and V.E. Henrich, Phys. Rev. B **38**, 5965 (1988)

[20] K.E. Smith and V.E. Henrich, Phys. Rev. B **38**, 9571 (1988)

[21] T. Uozumi, K. Okada, and A. Kotani, J. Phys. Soc. Jpn. **62**, 2595 (1993)

[22] T. Uozumi, K. Okada, A. Kotani, Y. Tezuka, and S. Shin, J. Phys. Soc. Jpn. **65**, 1150 (1996)

[23] R.L. Kurtz and V.E. Henrich, Surface Science Spectra **5**, 179 (1998)

[24] H. Sato, A. Tanaka, M. Sawada, F. Iga, K. Tsuji. M. Tsubota, M. Takemura, K. Yaji, M. Nagira, A. Kimura, T. Takabatake, H. Namatame, and M. Taniguchi, J. Phys. Soc. Jpn. **75**, 053702 (2006)

[25] N.W. Ashcroft and N.D. Mermin, *Solid State Physics*, Ch. 32, Problem 5 (Holt-Saunders, Tokyo, 1981)